

UNCLASSIFIED

AAEC/E 67

AUSTRALIAN ATOMIC ENERGY COMMISSION  
RESEARCH ESTABLISHMENT  
LUCAS HEIGHTS

PURIFICATION OF CARBON DIOXIDE FOR  
REACTOR PURPOSES  
PART II - PRESSURE LOSSES THROUGH PACKED  
BEDS OF SELECTED DESICCANTS

by

A. DRAYCOTT

A. C. KERR

Issued Sydney, May 1961



UNCLASSIFIED

AAEC/E 67



AUSTRALIAN ATOMIC ENERGY COMMISSION  
RESEARCH ESTABLISHMENT  
LUCAS HEIGHTS

PURIFICATION OF CARBON DIOXIDE FOR  
REACTOR PURPOSES

PART II - PRESSURE LOSSES THROUGH PACKED  
BEDS OF SELECTED DESICCANTS

by

A. DRAYCOTT

A. C. KERR

ABSTRACT

Pressure losses have been measured for the flow of carbon dioxide, air, argon, helium, hydrogen and methane through beds of molecular sieves, and for carbon dioxide and air through beds of activated alumina. It is shown that at the levels of moisture impurity expected in the Australian H.T.G.C. reactor no increased pressure loss caused by adsorption should be encountered. The effect of temperature was studied but in all cases found to be slight.

The coefficients  $a'$  and  $b$  in Ergun's modified equation

$$\frac{\Delta P}{LV_0} = a'\mu + bG$$

were calculated for all cases. Generally, good correlations were obtained although the low molecular weight gases, particularly hydrogen, showed considerable deviation.



## CONTENTS

	Page
1. INTRODUCTION	1
2. THEORY	1
2.1 Packing Variables	2
2.2 Pressure Losses in Beds Accompanied by Adsorption	3
3. EXPERIMENTAL METHOD	3
4. RESULTS	4
4.1 Molecular Sieves	4
4.2 Activated Alumina	5
5. CONCLUSIONS	6
6. REFERENCES	7
7. NOTATION	7
Table 1 Pressure loss due to water vapour adsorption	8
Table 2 Values of a' and b obtained with molecular sieves	9
Table 3 Values of a' and b obtained with -6 + 8 mesh alumina	10
Table 4 Values of a' and b obtained with -5 + 6 mesh alumina	11
Table 5 Values of a' and b obtained with $\frac{-3}{16}$ inch + 5 mesh alumina	11
Figure 1 Schematic diagram of experimental equipment	
Figure 2 Plot $\frac{\Delta P}{LV_0}$ versus G for molecular sieves; fluid, air at 23°C	
Figure 3 Temperature effect on pressure loss through molecular sieves; fluid, air at 55°C and 103°C	
Figure 4 Temperature effect on pressure loss through molecular sieves; fluid, carbon dioxide at 61°C and 88°C	
Figure 5 Temperature effect on pressure loss through molecular sieves; fluid, argon at 23°C and 71°C	
Figure 6 Plot $\frac{\Delta P}{LV_0}$ versus G for -6 + 8 mesh alumina; fluid, air at 23°C	
Figure 7 Plot $\frac{\Delta P}{LV_0}$ versus G for -6 + 8 mesh alumina; fluid, carbon dioxide at 23°C	

(Continued)

CONTENTS (continued)

- Figure 8 Plot  $\frac{\Delta P}{LV_0}$  versus G for -6 +8 mesh alumina; fluid, carbon dioxide at 55°C
- Figure 9 Plot  $\frac{\Delta P}{LV_0}$  versus G for -6 +8 mesh alumina; fluid, carbon dioxide at 100°C
- Figure 10 Variation of a' with bulk density for alumina -6 +8 mesh
- Figure 11 Variation of b with bulk density for alumina -6 +8 mesh
- Figure 12 Plot  $\frac{\Delta P}{LV_0}$  versus G for -5 +6 mesh alumina; fluid, air at 22°C
- Figure 13 Plot  $\frac{\Delta P}{LV_0}$  versus G for -5 +6 mesh alumina; fluid, carbon dioxide at 23°C
- Figure 14 Variation of a' with bulk density for alumina -5 +6 mesh
- Figure 15 Variation of b with bulk density for alumina -5 +6 mesh
- Figure 16 Plot  $\frac{\Delta P}{LV_0}$  versus G for  $-\frac{3}{16}$  in. +5 mesh alumina; fluid, air at 23°C
- Figure 17 Variation of a' with bulk density for alumina  $-\frac{3}{16}$  in. +5 mesh
- Figure 18 Variation of b with bulk density for alumina  $-\frac{3}{16}$  in. +5 mesh

## 1. INTRODUCTION

The first part of the programme of work recommended in Part I (Draycott and Kerr, 1960) has been completed. This report describes the work on the pressure loss accompanying the flow of gases through the selected desiccants, molecular sieves, and activated alumina. Though carbon dioxide is the favoured coolant for the Australian H.T.G.C. reactor, opportunity was taken to measure the pressure losses with gases of widely different molecular weight and viscosity and to attempt a correlation.

## 2. THEORY

In the past, pressure losses due to the flow of a gas through packed beds of granular material have been the subject of both theoretical analyses and experimental investigations. Beds containing solids of uniform geometric shape have received the most attention. Molecular sieves are usually supplied in cylindrical form of uniform diameter with some little variation in length. Some experiments have been carried out on the flow of gas through crushed porous solids, as this is the case most commonly met in practice and applies where alumina is the desiccant.

Many factors are involved in determining the pressure drop through packed beds and some are difficult to analyse mathematically. Usually many simplifying assumptions are made to correlate the experimental data. The main factors to be considered appear to be:

- (1) rate of fluid flow,
- (2) viscosity and density of the fluid,
- (3) porosity of the packing, and
- (4) size, shape and surface of the packing.

Chilton and Colburn (1931), Carman (1937) and Leva and Grummer (1947) found it impossible to correlate their experimental data over the complete range of Reynolds' numbers studied. Two equations were obtained, one for streamline and the other for turbulent flow.

Carman's (1937) correlation can be expressed in the following way:

$$\Delta P = \frac{f_c L S \rho_G V_o^2}{g \epsilon^3} \quad \text{for } Re > 10 \quad (1)$$

$$\begin{aligned} \Delta P &= \frac{5\mu L S^2 V_o}{g \epsilon^3} \\ &= \frac{180\mu L (1-\epsilon)^2 V_o}{g \epsilon^3 \phi^2 D_p^2} \quad \text{for } Re < 2 \quad (2) \end{aligned}$$

where  $f_c$  is a friction factor dependent on a modified Reynolds' number defined as

$$Re = \frac{\phi D_p V_o \rho_G}{6\mu(1-\epsilon)}$$

The size  $D_p$  and shape factor  $\phi$  proved the most difficult to determine accurately.

Reynolds (1900) was the first to postulate that pressure losses could be equated to the sum of simultaneous kinetic and viscous energy losses. We therefore have

$$\frac{\Delta P}{L} = aV_o + b\rho_G V_o^2 \quad (3)$$

a and b being factors which are functions of the system.

The mass flow  $G = \rho_G V_o$  and equation (3) now becomes linear of the form

$$\frac{\Delta P}{LV_o} = a + bG \quad (4)$$

This equation has been tested experimentally by several workers including Ergun and Orning (1949) and found to express accurately the relationship between flow rate and pressure drop. Factor a is proportional to viscosity of the fluid.

$$\text{Thus } \frac{\Delta P}{LV_o} = a'\mu + bG \quad (5)$$

where  $a' = \frac{a}{\mu}$ .

Equation (5) contains factors which are properties of the fluid and can therefore be used for any gas but is specific for a particular bed packing.

### 2.1 Packing Variables

Burke and Plummer (1928) and Leva and Grummer (1947) have indicated that the pressure drop through a packed bed depends upon the void volume and subsequently Ergun and Orning (1949) stated

$$a = \frac{A(1-\epsilon)^2}{\epsilon^3} \quad (6)$$

$$\text{and } b = \frac{B(1-\epsilon)}{\epsilon^3} \quad (7)$$

where A and B are further constants. These equations have been proved experimentally by Ergun (1952) for nitrogen flow through -16 + 20 mesh coke. For any particular system A and B must be determined by experiment.

Ergun and Orning (1949) further developed an equation to allow for particle size and shape:

$$\frac{\Delta P_G}{LV_o} = 2\alpha\mu S^2 \frac{(1-\epsilon)^2}{\epsilon^3} \left(\frac{\beta}{8}\right) GS \frac{(1-\epsilon)}{\epsilon^3} \quad (8)$$

where  $\alpha$  and  $\beta$  are constants.

If we use the characteristic dimension  $D_p$ , the diameter of a sphere having the specific surface S, the equation becomes

$$\frac{\Delta P_G}{LV_o} = k_1 \frac{(1-\epsilon)^2}{\epsilon^3} \frac{\mu}{D_p^2} + k_2 \frac{1-\epsilon}{\epsilon^3} \frac{G}{D_p} \quad (9)$$

Determination of S, the specific surface area, involves measurement of the solid surface area, and obviously presents a problem with irregular porous materials. It is thus the limiting feature of the equation.

## 2.2 Pressure Losses in Beds Accompanied by Adsorption

In all the considerations above, no account has been taken of any change in composition of the gas due to adsorption of one or more constituents. In some cases the pressure loss accompanying such adsorption may be appreciable and must be evaluated.

The pressure loss in a packed column in which adsorption occurs may be divided into the following three categories:

- (a) Pressure loss in the saturated zone due to flow of inert gas and adsorbate.
- (b) Pressure loss in mass transfer zone due to:
  - (i) change in adsorbate concentration,
  - (ii) change in volume of inert gas as adsorbate is removed.
- (c) Pressure loss in unsaturated zone due to flow of inert gas alone.

The total pressure loss in an adsorption cycle varies with time, as does the throughput, the relationship between these variables being rather complex. In our case it was shown that if the change of moisture content of the carbon dioxide is of the order of 100 p.p.m. the variation in pressure loss is negligible.

In Table 1 for a typical set of conditions the increased pressure loss due to water vapour adsorption is shown as a function of inlet moisture content and total pressure of air in a bed 10 feet long and superficial gas velocity of 1.5 ft/sec. The gas is assumed to expand to its inlet volume at the column outlet.

This clearly demonstrates that under the conditions expected, even if the working pressure reaches 300 p.s.i.g., little increase in pressure loss due to water vapour adsorption occurs.

## 3. EXPERIMENTAL METHOD

A schematic diagram of the apparatus used is shown in Figure 1. The gas being tested passed through a rotameter, then a pre-heater (hot runs only) and flowed up through the bed of desiccant. The range of flows tested was 2 to 10 lb/(ft<sup>2</sup>) (min). Carbon dioxide, air, argon, helium, hydrogen, and methane were examined using molecular sieve desiccant, and only carbon dioxide and air were tested using activated alumina. The molecular sieves, Linde Type 4A, were of uniform diameter of 1/8 inch and nominal length of approximately 3/16 inch. Three size fractions of alumina were examined. These were:

- 3/16 inch + 5 mesh BSS
- 5 + 6 mesh BSS
- 6 + 8 mesh BSS

The bed was contained in a glass tube 2 feet 6 inches long and 1½ inch diameter. Lengths of bed in experiments with air varied from 10 to 28 inches. In most other cases only one bed length was used as the pressure drop was found to be directly proportional to this variable. Two pressure tappings were fitted. These enabled pressure drop across the bed and downstream gas pressure to be measured.

Most experiments were done at room temperature but to determine the effect of temperature it was varied in some experiments on carbon dioxide, air, and argon. The temperatures used in these cases were:

CO<sub>2</sub> - 23°C (Room Temp.), 55°C, and 100°C with alumina, and 61°C and 88°C with molecular sieves.

Air - 23°C, 55°C and 103°C with molecular sieves.

Argon - 23°C and 71°C with molecular sieves.

These figures quoted are means of measurements obtained from two mercury-in-glass thermometers placed at the top and bottom of the bed respectively.

#### 4. RESULTS

##### 4.1 Molecular Sieves

Because of the uniform diameter of the molecular sieves it was found that under normal conditions the void volume varied only within narrow limits (bulk densities by between 55.0 and 56.5 lb/ft<sup>3</sup>). Therefore, it was not necessary to take account of packing variables and the main study was directed towards the evaluation of the constants in

$$\frac{\Delta P}{LV_0} = a'\mu + bG.$$

From the measured values of flow rate, pressure drop across the bed, the bed length, inlet pressure of the column, and temperature, the terms  $\frac{\Delta P}{LV_0}$  and G were calculated.

In Figure 2  $\frac{\Delta P}{LV_0}$  is plotted against G for air at 23°C. All the experimental points have been included. The relationship is clearly linear. The effect of temperature for this fluid, as shown in Figure 3 is very small as was expected. Similar graphs for carbon dioxide and argon at two temperatures are shown in Figures 4 and 5.

The straight lines shown in these figures were obtained using the method of least squares. From these the coefficients a' and b for all the gases were evaluated as given in Table 2. This table clearly demonstrates that the pressure loss characteristics through packed bed of molecular sieves, of the low molecular weight gases differ markedly from those of carbon dioxide, air, and argon.

The values of the coefficients a' and b for air, argon and carbon dioxide are very similar. No distinct trend in a' with temperature was observed for any gas, but the values of b generally decreased with increase in temperature. The results for air, argon and carbon dioxide can be satisfactorily summarised by the following equation:

$$\frac{\Delta P}{LV_0} = 4100 \mu + 0.015 G. \quad (10)$$

Column 5 of Table 2 shows the average errors entailed by the use of this equation for calculation of pressure losses for these gases through beds of molecular sieve pellets 1/8 inch in diameter.

The deviation of b values in equation (5) is most marked in the case of hydrogen, becoming less as the molecular weight increases through helium to methane. However, the a' coefficient for hydrogen is closer to those for the other gases than the corresponding coefficients for helium and methane. No explanation is apparent for these deviations.

Pressure losses through any bed of 1/8 inch molecular sieves can be calculated using the equation developed for each gas. In no cases should the errors involved greatly exceed 10 per cent.

#### 4.2 Activated Alumina

Because of the varying size and shape of the alumina particles, bulk density was an important parameter which had to be considered. Air and carbon dioxide were the only gases used in the experiments on alumina. In both cases the experiments were completed at different temperatures. The standard plots of  $\frac{\Delta P}{LV_0}$  against G for varying bulk densities, for both gases at different temperatures are shown in Figures 6 to 9 with alumina of size range -6+8 mesh BSS. In all cases good linearity was observed.

The values of coefficients a' and b obtained from these plots by the method of least squares are shown in Table 3.

As indicated in Section 2, Ergun and Orning (1949) showed that

$$a' \propto \frac{(1-\epsilon)^2}{\epsilon^3}$$

and

$$b \propto \frac{1-\epsilon}{\epsilon^3}$$

It can be shown that over the range of void volumes normal for alumina (0.46 to 0.50),

$$\rho_b \propto \frac{(1-\epsilon)^2}{\epsilon^3} \quad \text{and} \quad \rho_b \propto \frac{1-\epsilon}{\epsilon^3}$$

within 0.7 per cent. This has resulted in a considerable simplification of Ergun and Orning's (1949) correlation without sacrificing accuracy.

In Figure 10, a' is plotted against  $\rho_b$  and the following relationship is obtained:

$$a' = 530 \rho_b - 23750, \quad (11)$$

while in Figure 11, b is plotted against  $\rho_b$  and we obtain

$$b = 0.00104 \rho_b - 0.0440 \quad (12)$$

for the size range of alumina under consideration.

The accuracy of these equations in predicting the drop through beds of -6+8 mesh BSS alumina was checked over 201 runs in the experimental investigation. The average error involved was 4.7 per cent.

The other size ranges were considered in a similar manner, but not so extensively, as the method of correlation was satisfactorily proved with the -6+8 mesh BSS alumina.

The results for these size ranges are presented in Tables 4 and 5 and in Figures 12, 13 and 16. The relationships between  $a'$ ,  $b$ , and  $\rho_b$  obtained for the size ranges  $-3/16$  in. + 5 mesh and  $-5+6$  mesh BSS were as follows:

Size Range:  $-5+6$  mesh BSS

$$b = 0.00114 \rho_b - 0.0492 \quad (\text{See Figure 14}) \quad (13)$$

$$a' = 510 \rho_b - 23400 \quad (\text{See Figure 15}) \quad (14)$$

Size Range:  $-3/16$  in. + 5 mesh BSS

$$b = 0.00117 \rho_b - 0.0523 \quad (\text{See Figure 17}) \quad (15)$$

$$a' = 550 \rho_b - 25,100 \quad (\text{See Figure 18}) \quad (16)$$

The average error involved in the use of these equations for estimating the pressure losses through beds of these materials is 3.4 per cent. and was found never to exceed 7.6 per cent. in the range of variables studied.

No correlation including particle size and shape is proposed. However, the above results cover a considerable size distribution and particularly the size ranges of desiccants used in practice.

Thus having the size range and bulk density of the bed using the above correlations, pressure losses can be calculated for a particular bed under specified operating conditions with a sufficient degree of accuracy.

## 5. CONCLUSIONS

At the levels of moisture impurity expected in the Australian H.T.G.C. reactor no increased pressure loss caused by adsorption should be encountered.

The coefficients  $a'$  and  $b$  in the modified Ergun's equation

$$\frac{\Delta P}{LV_0} = a'\mu + bG$$

determined for the flow of a number of gases through beds of molecular sieves and activated alumina are listed.

For molecular sieves, low molecular weight gases, hydrogen, helium and methane deviate from the general correlation developed for other gases. This correlation enables pressure losses to be calculated with errors not exceeding 10 per cent. In all cases, the effect of temperature is slight. The values of  $a'$  and  $b$  obtained at different temperatures for air, argon and carbon dioxide are given.

For each size range of activated alumina separate correlations were obtained. It was not possible to get any correlation incorporating particle size and shape because of the restricted size range studied. However, the particle size ranges examined are those most likely to be used in practical applications of alumina as a desiccant.

## 6. REFERENCES

- Burke, S.P., and Plummer, W.B., (1928). Gas flow through packed columns. *Ind. Eng. Chem.* 20: 1196.
- Carman, P.C., (1937). Fluid flow through granular beds. *Trans. Inst. Chem. Engrs. (London)* 15: 150.
- Chilton, T.H., and Colburn, A.P., (1931). Pressure drop in packed tubes. *Ind. Eng. Chem.* 23: 913.
- Draycott, A., and Kerr, A.C., (1960). Purification of carbon dioxide for reactor purposes.  
Part I - AAEC/E 58.
- Ergun, S., (1952). Fluid flow through packed columns. *Chem. Eng. Prog.* 48: 89.
- Ergun, S., and Orning, A.A., (1949). Fluid flow through randomly packed columns and fluidized beds.  
*Ind. Eng. Chem.* 41: 1179.
- Leva, M., and Grummer, M., (1947). Pressure drop through packed tubes. *Chem. Eng. Prog.* 43: 549,  
633, 713.
- Reynolds, O., (1900). Papers on mechanical and physical subjects. Cambridge University Press.

## 7. NOTATION

- a coefficient of viscous energy term in Equation 3
- $a' = a/\mu$ , a constant
- b coefficient of kinetic energy term in Equation 3
- A constant in Equation 6
- B constant in Equation 7
- $D_p$  effective particle diameter; ft.
- $f_c$  friction factor; dimensionless
- G mass flow rate; lb/(ft<sup>2</sup>) (min)
- g gravitational constant
- $k_1$  coefficient of viscous energy term in Equation 9
- $k_2$  coefficient of kinetic energy term in Equation 9
- L height of bed; ft.
- $\Delta P$  pressure loss; lb/ft<sup>2</sup>
- S surface of solids per unit volume of bed; ft<sup>2</sup>/ft<sup>3</sup>
- $V_o$  superficial fluid velocity measured at average temperature and pressure; ft/min
- $\alpha$  coefficient of viscous energy term in Equation 8

- $\beta$  coefficient of kinetic energy term in Equation 8
- $\epsilon$  fractional void volume in bed
- $\mu$  absolute viscosity of fluid; lb(mass)/(ft)(sec)
- $\rho_G$  density of fluid; lb/ft<sup>3</sup>
- $\rho_b$  bulk density of the packing; lb/ft<sup>3</sup>
- $\phi$  shape factor of the packing

TABLE 1

Pressure Loss due to Water Vapour Adsorption

Nominal bed length – 10 ft.

Superficial gas velocity – 1.5 ft/sec.

Pressure loss without adsorption – 50 mm Hg.

Inlet Concentration of H <sub>2</sub> O p.p.m.	Pressure loss due to adsorption alone (mm Hg) at the following absolute pressure – atmospheres				
	1	2	5	10	20
100	0.07	0.14	0.35	0.70	1.40
500	0.38	0.76	1.9	3.8	7.6
1000	0.76	1.5	3.8	7.6	15.2
5000	3.8	7.6	19	38	76

**TABLE 2**

Values of a' and b Obtained with Molecular Sieves

Gas	Temp.	a'	b	Errors
Air	23°C	4680	0.016	
	55°C	4650	0.015	5.7%
	103°C	4450	0.015	4.2%
CO <sub>2</sub>	27°C	4300	0.015	
	61°C	3700	0.014	11.8%
	88°C	3850	0.014	11.8%
Argon	23°C	3650	0.017	2.8%
	71°C	3850	0.014	7.1%
Hydrogen	25°C	4250	0.039	
Helium	25°C	2140	0.030	
Methane	25°C	2100	0.025	

**TABLE 3**

Values of a' and b Obtained with -6 +8 Mesh Alumina

Gas	Bulk Density	Temp.	a'	b
Air	50.4	23°C	3140	0.083
	51.3		3470	0.092
	52.2		3800	0.109
	53.0		4100	0.115
	53.2		4400	0.108
	53.6		4960	0.125
CO <sub>2</sub>	50.0	22°C	2890	0.083
		55°C	3560	0.073
		95°C	2700	0.081
	52.0	23°C	4050	0.099
		55°C	3700	0.086
		102°C	3400	0.090
	54.2	55°C	5200	0.125
		102°C	5600	0.116
		56.0	23°C	6300
102°C	6100		0.130	

**TABLE 4**

Values of a' and b Obtained with -5 +6 Mesh Alumina

	$\rho_b$	a'	b
CO <sub>2</sub>	50.0	2250	0.082
	52.6	3460	0.102
	55.6	5250	0.146
	56.8	5620	0.153
Air	56.2	5360	0.150

**TABLE 5**

Values of a' and b Obtained with -3/16 +5 Mesh Alumina

	$\rho_b$	a'	b
Air	51.2	2940	0.079
	52.4	3590	0.081
	53.7	4240	0.103
	54.2	4620	0.113



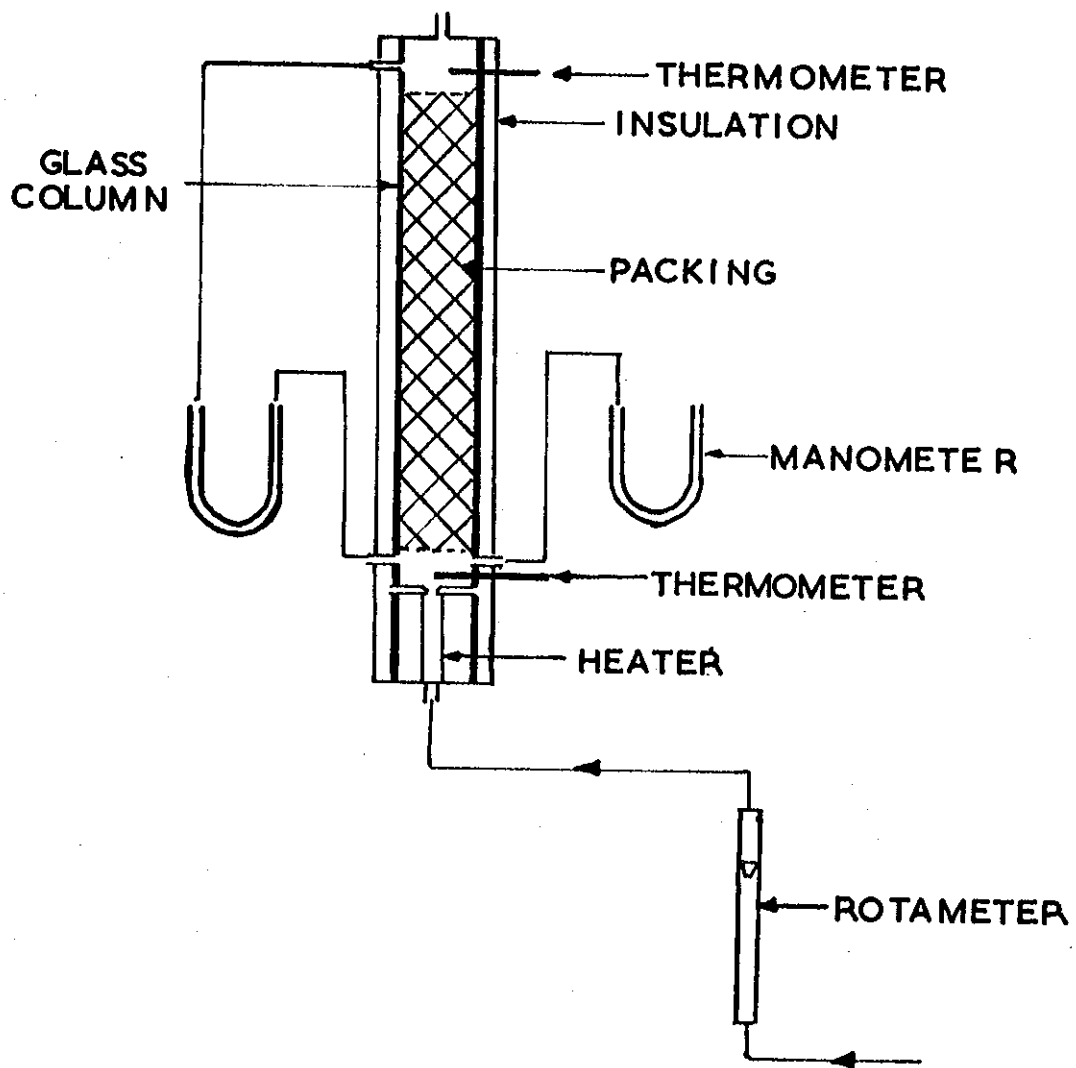


FIG 1  
SCHEMATIC DIAGRAM OF  
EXPERIMENTAL EQUIPMENT

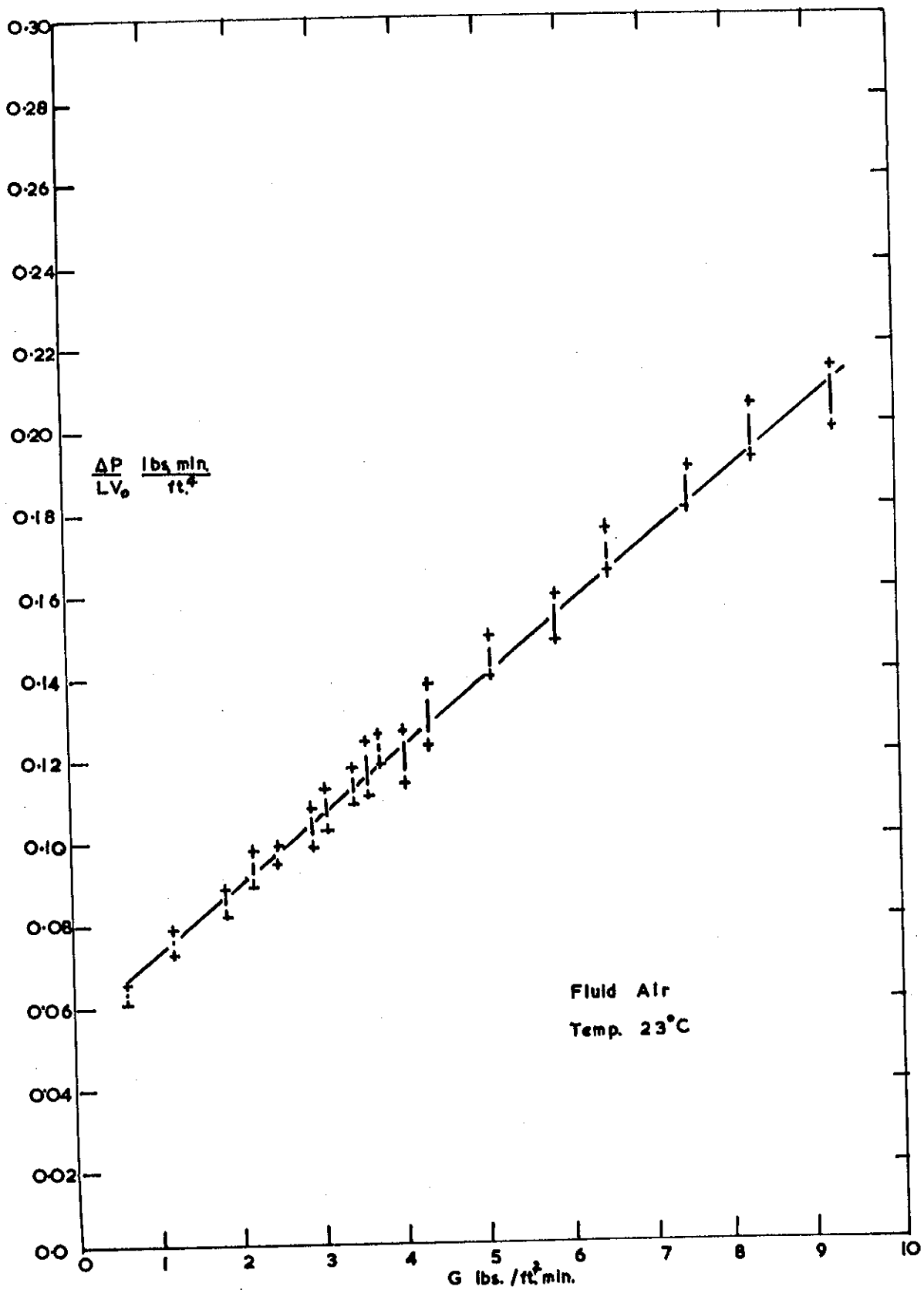


FIG. 2

PLOT  $\frac{\Delta P}{LV_0}$  VERSUS G FOR MOLECULAR SIEVES

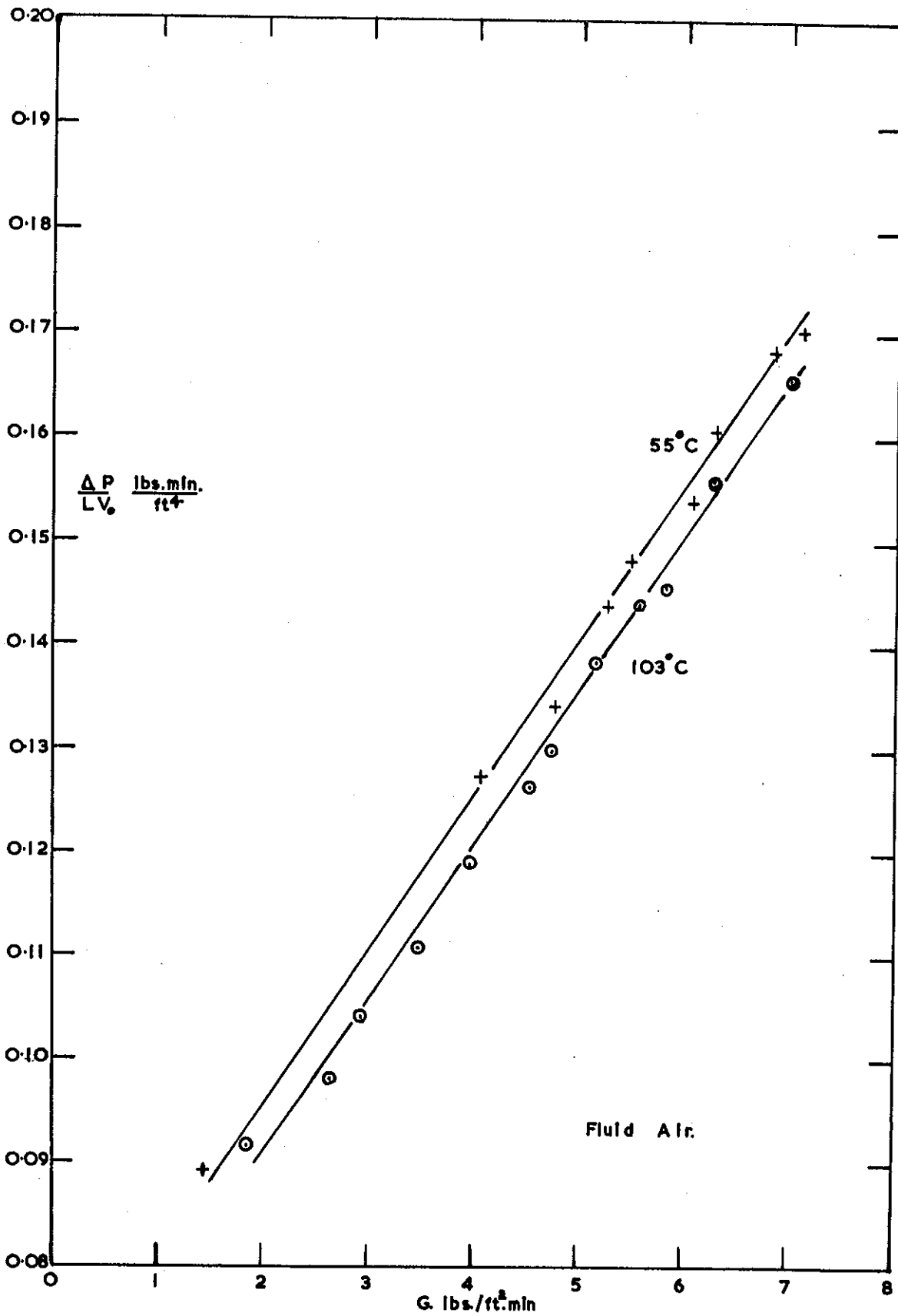


FIG. 3

TEMPERATURE EFFECT ON PRESSURE LOSS THROUGH MOLECULAR SIEVES

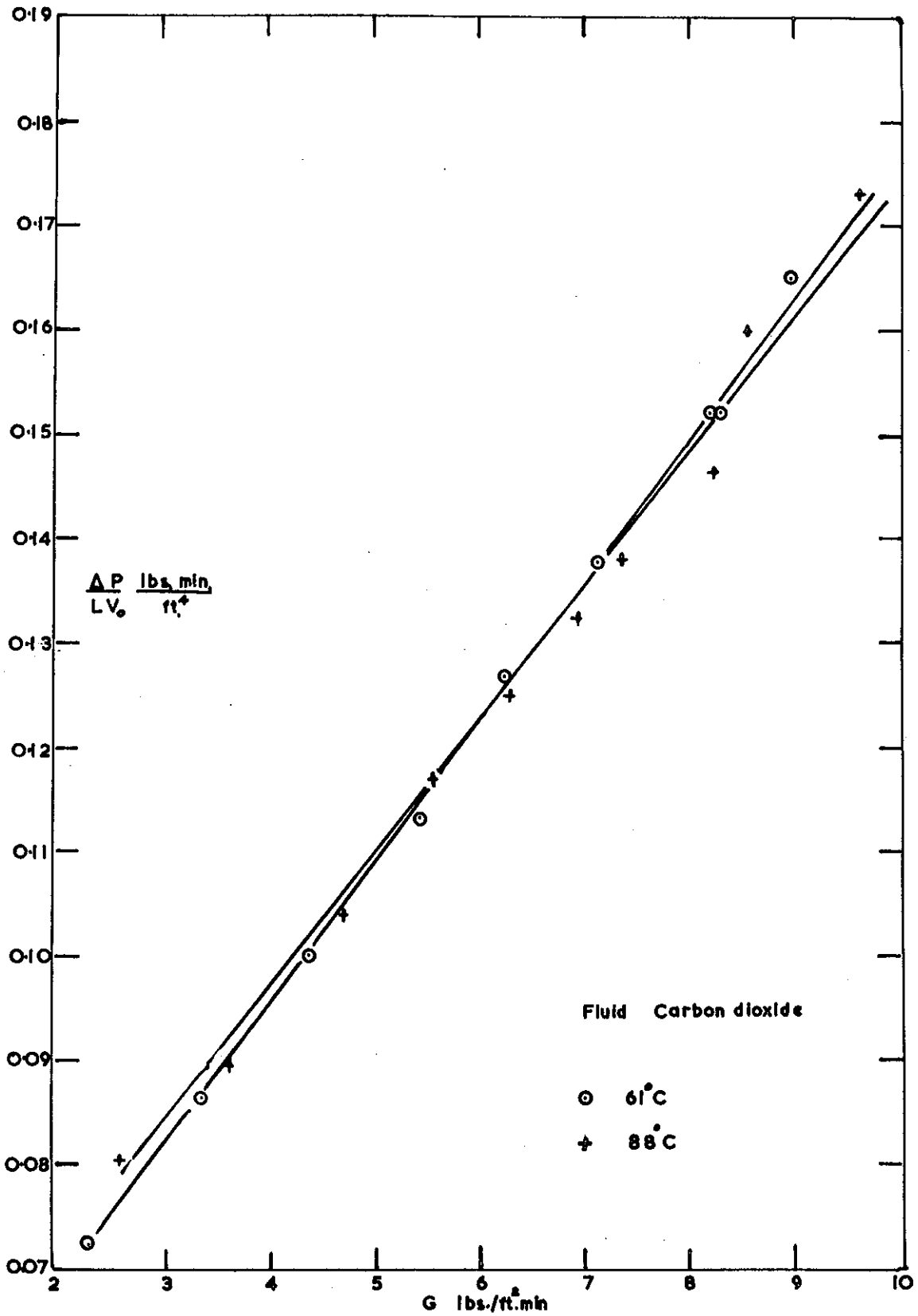


FIG. 4

TEMPERATURE EFFECT ON PRESSURE LOSS THROUGH MOLECULAR SIEVES.

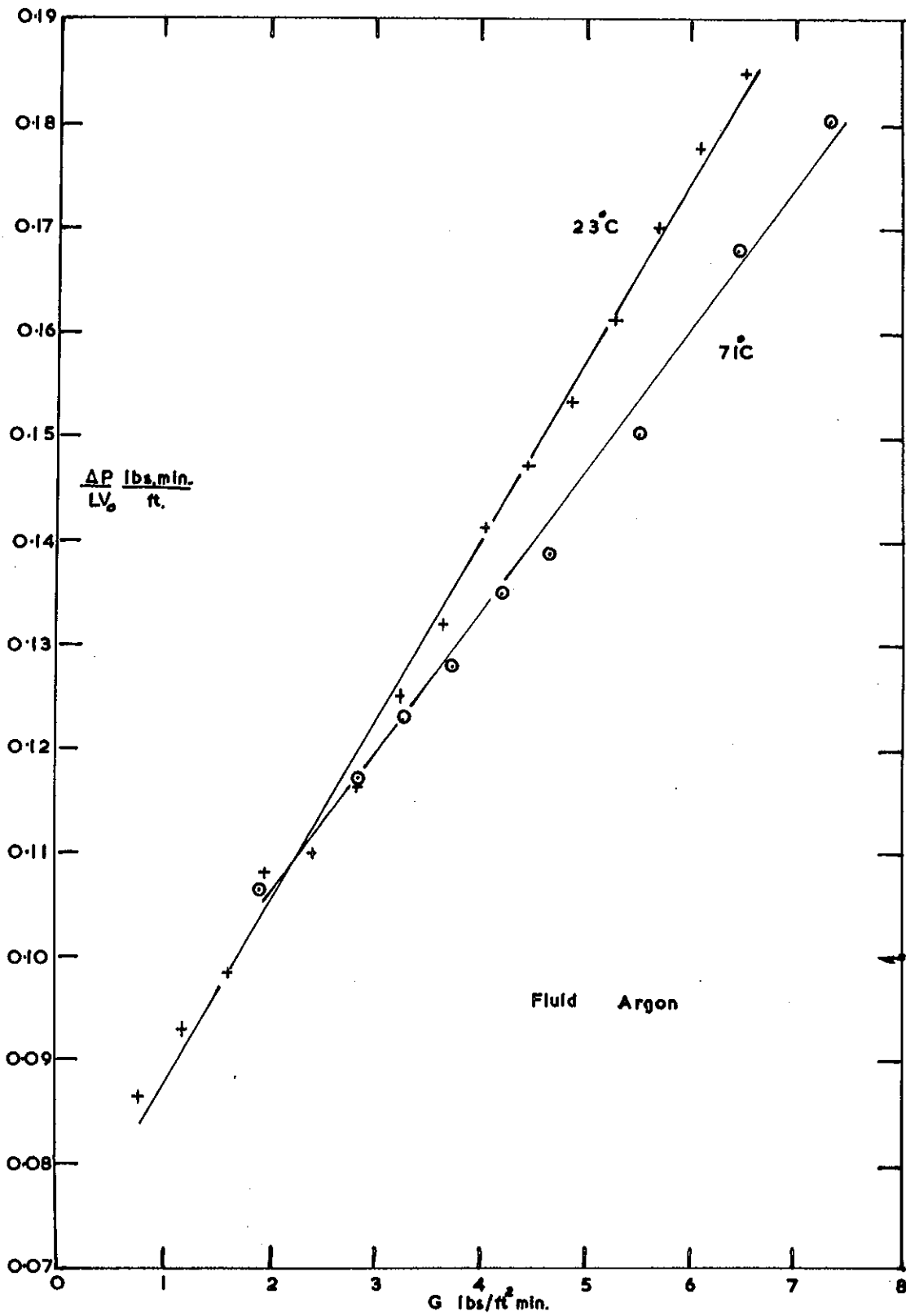


FIG. 5  
 TEMPERATURE EFFECT ON PRESSURE LOSS THROUGH  
 MOLECULAR SIEVES.

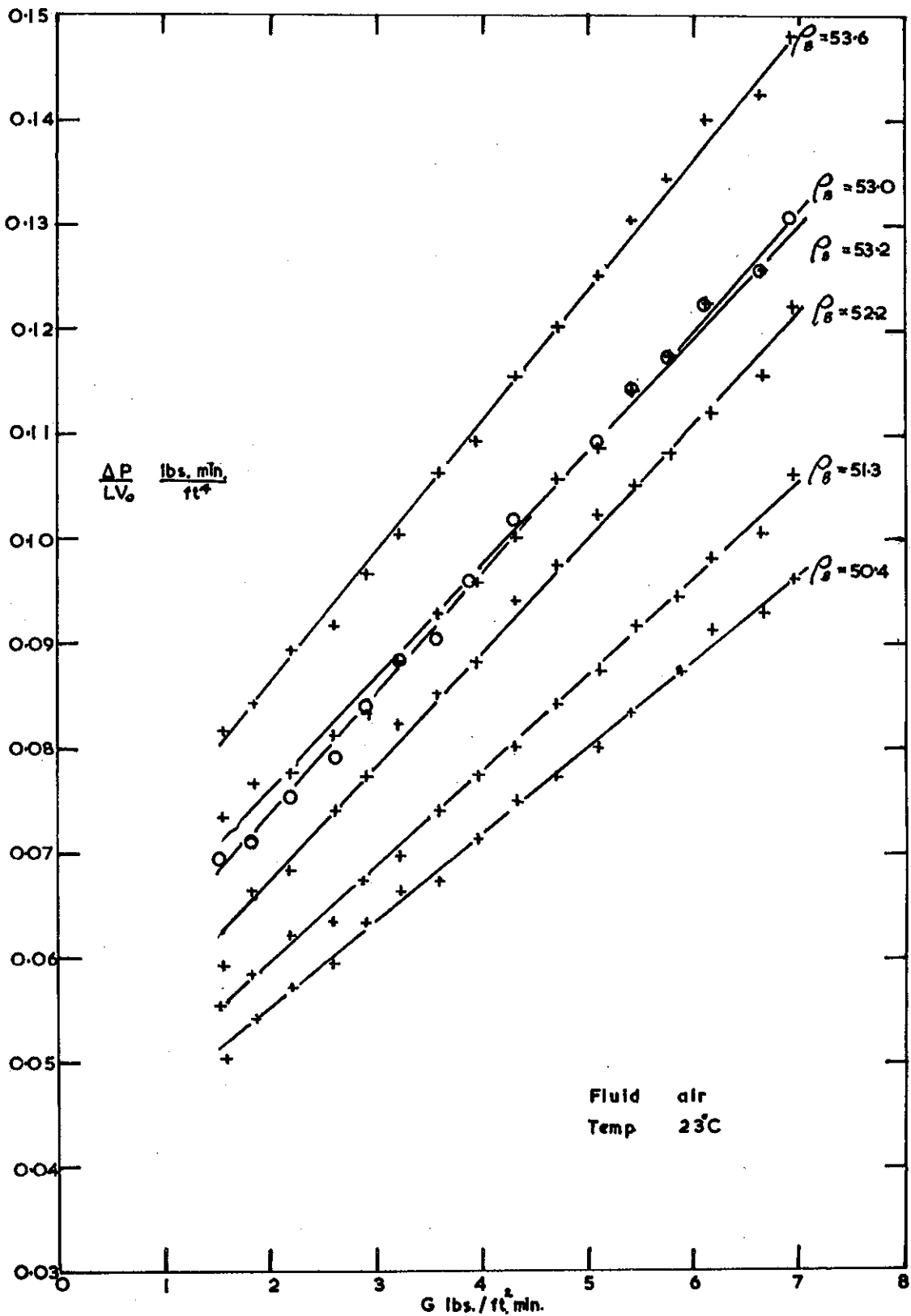


FIG. 6

PLOT  $\frac{\Delta P}{LV_0}$  VERSUS G FOR -6 + 8 MESH ALUMINA.

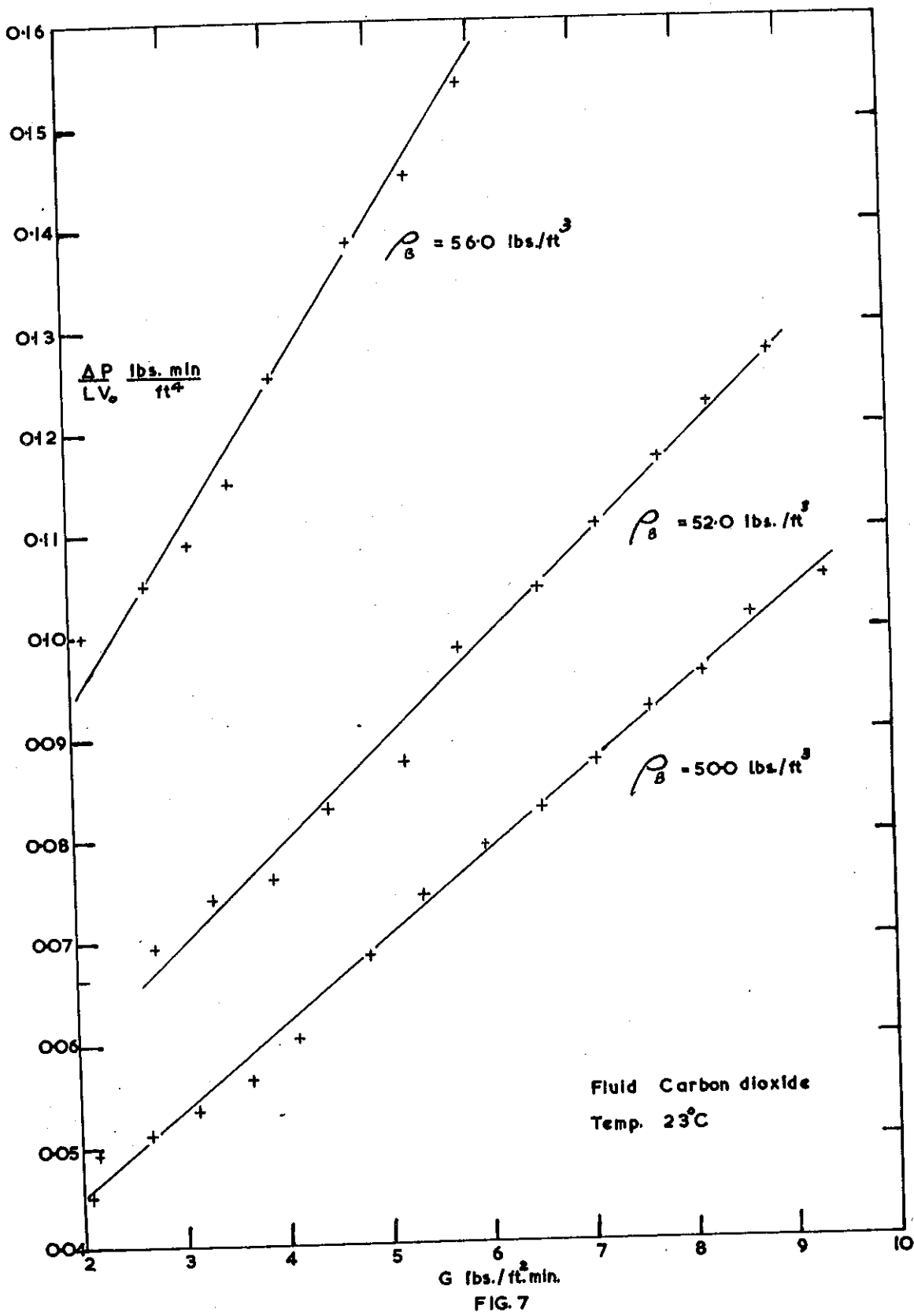


FIG. 7  
 PLOT  $\frac{\Delta P}{LV_0}$  VERSUS G FOR -6 + 8 MESH ALUMINA.

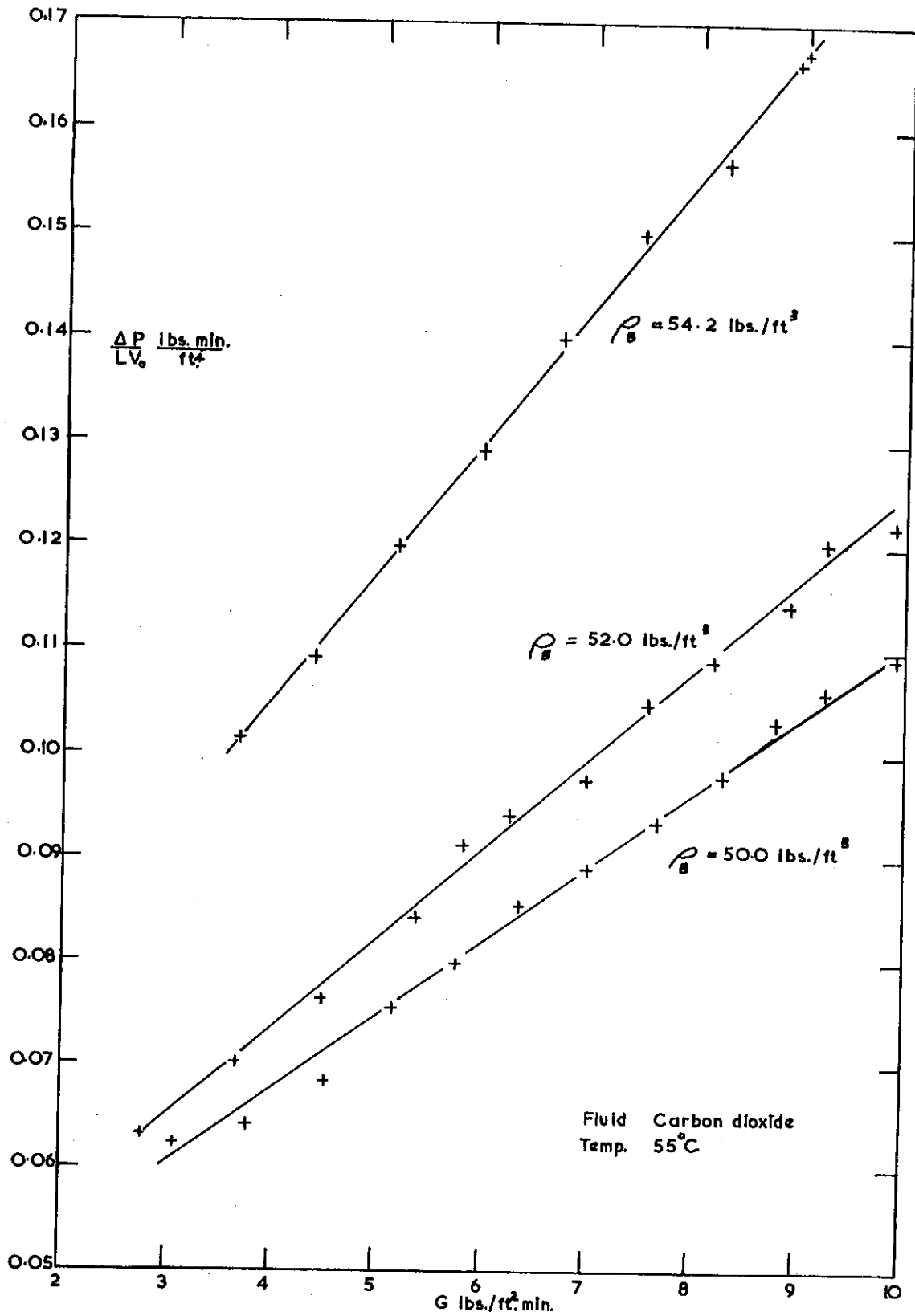


FIG. 8

PLOT  $\frac{\Delta P}{LV_0}$  VERSUS G FOR -6+8 MESH ALUMINA.

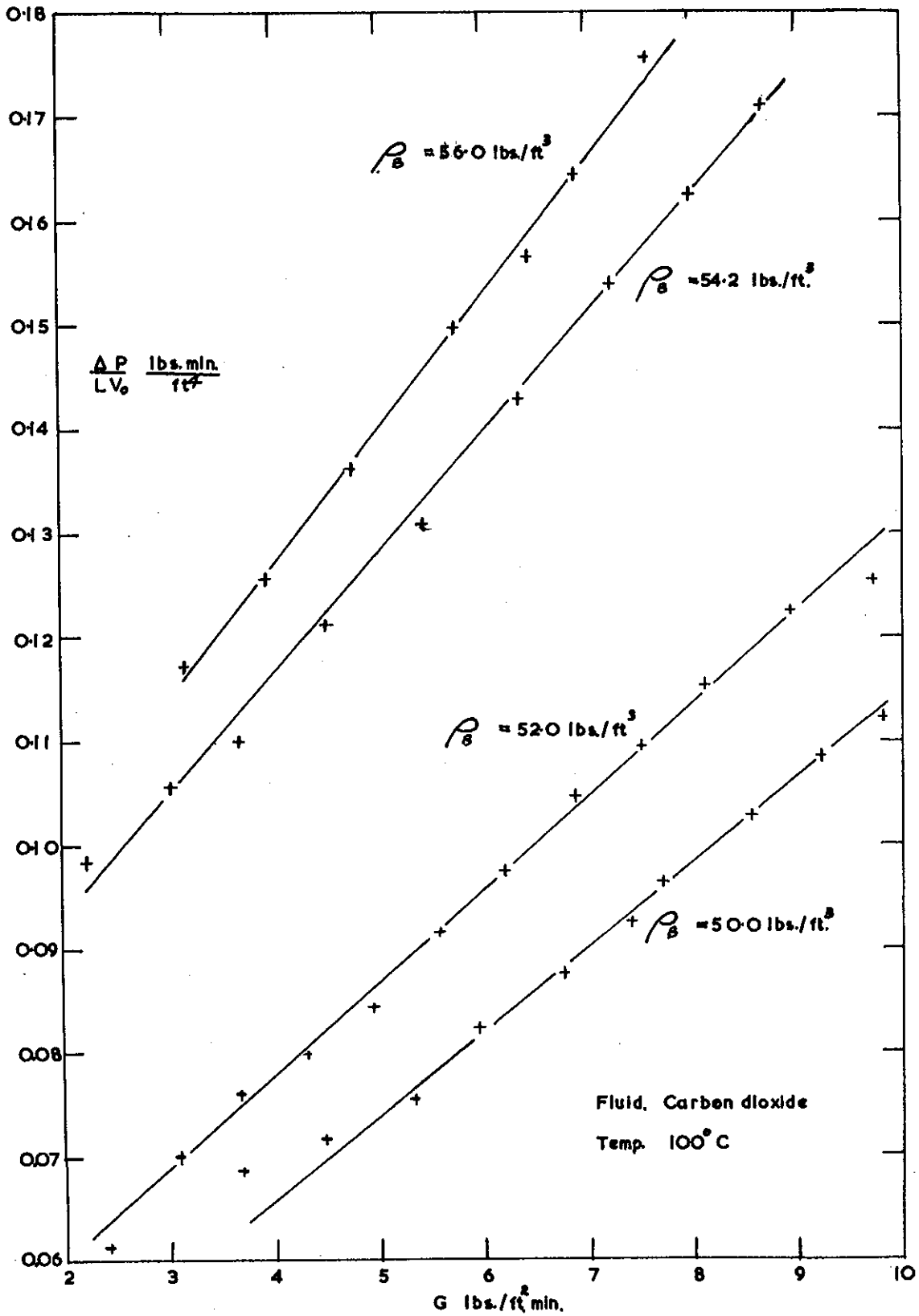


FIG. 9  
 PLOT  $\frac{\Delta P}{LV_0}$  VERSUS G FOR -6 + 8 MESH ALUMINA.

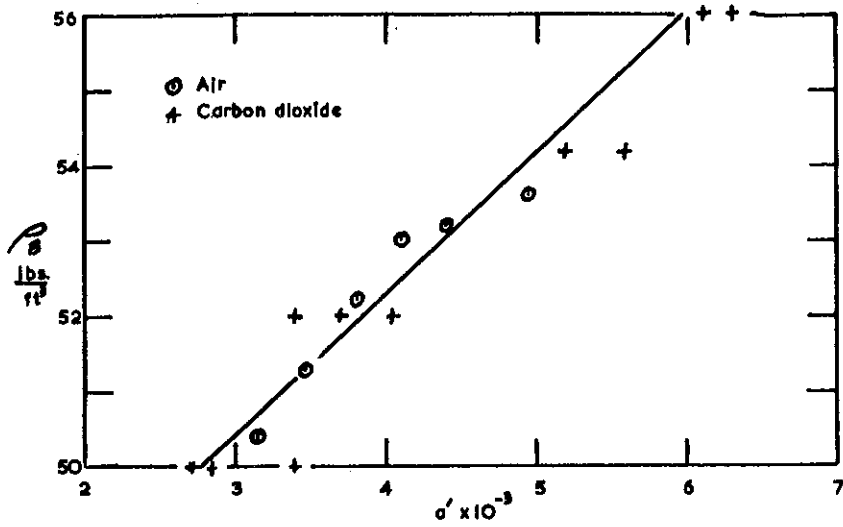


FIG. 10

VARIATION of  $\sigma'$  WITH BULK DENSITY for ALUMINA -6+8 MESH

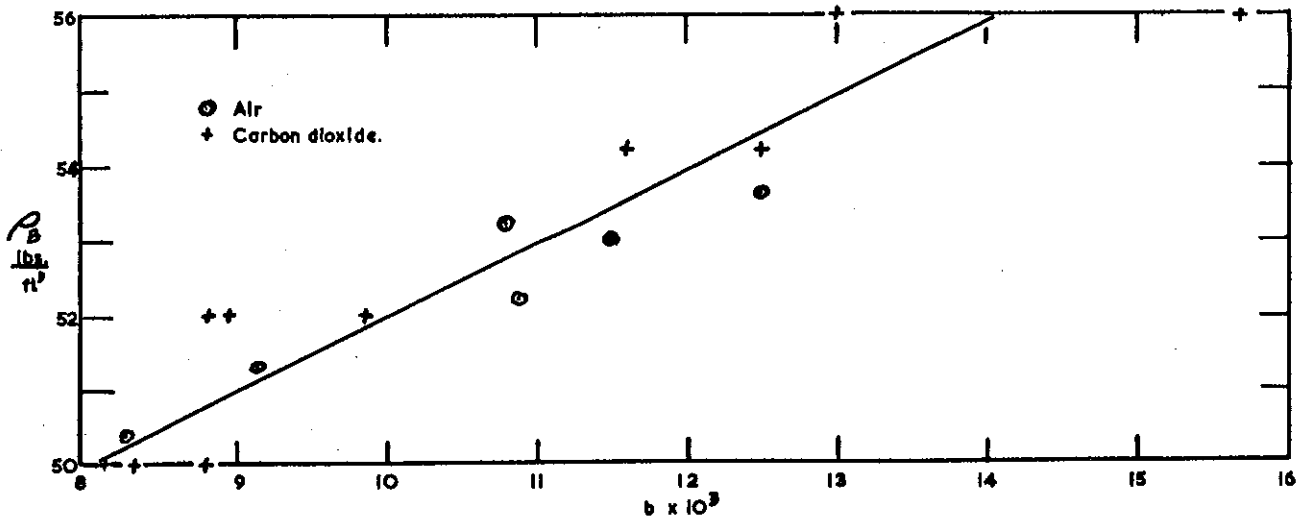


FIG. 11.

VARIATION of  $b$  WITH BULK DENSITY for ALUMINA -6+8 MESH

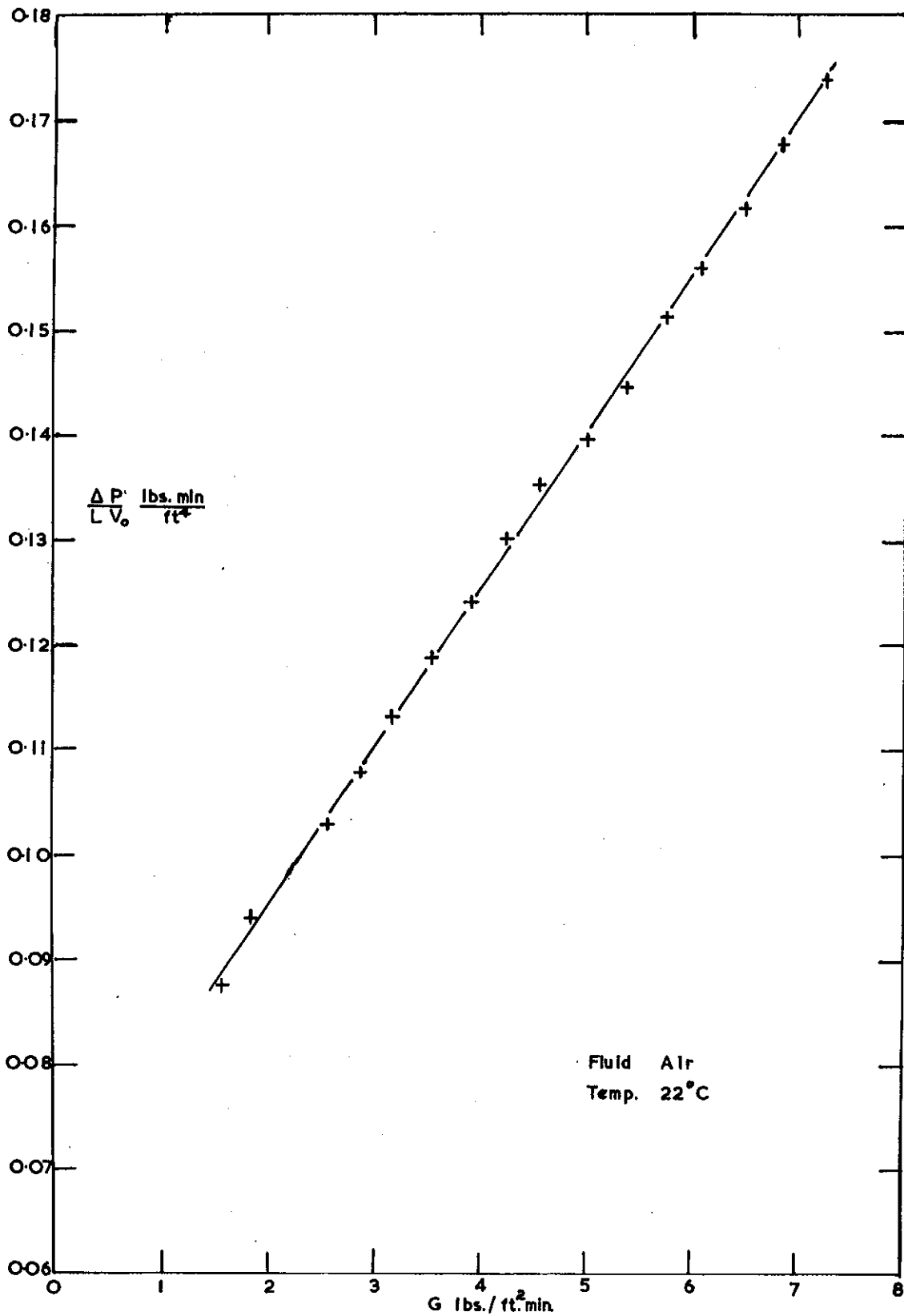


FIG. 12

PLOT  $\frac{\Delta P}{L V_0}$  VERSUS G FOR -5 + 6 MESH ALUMINA.

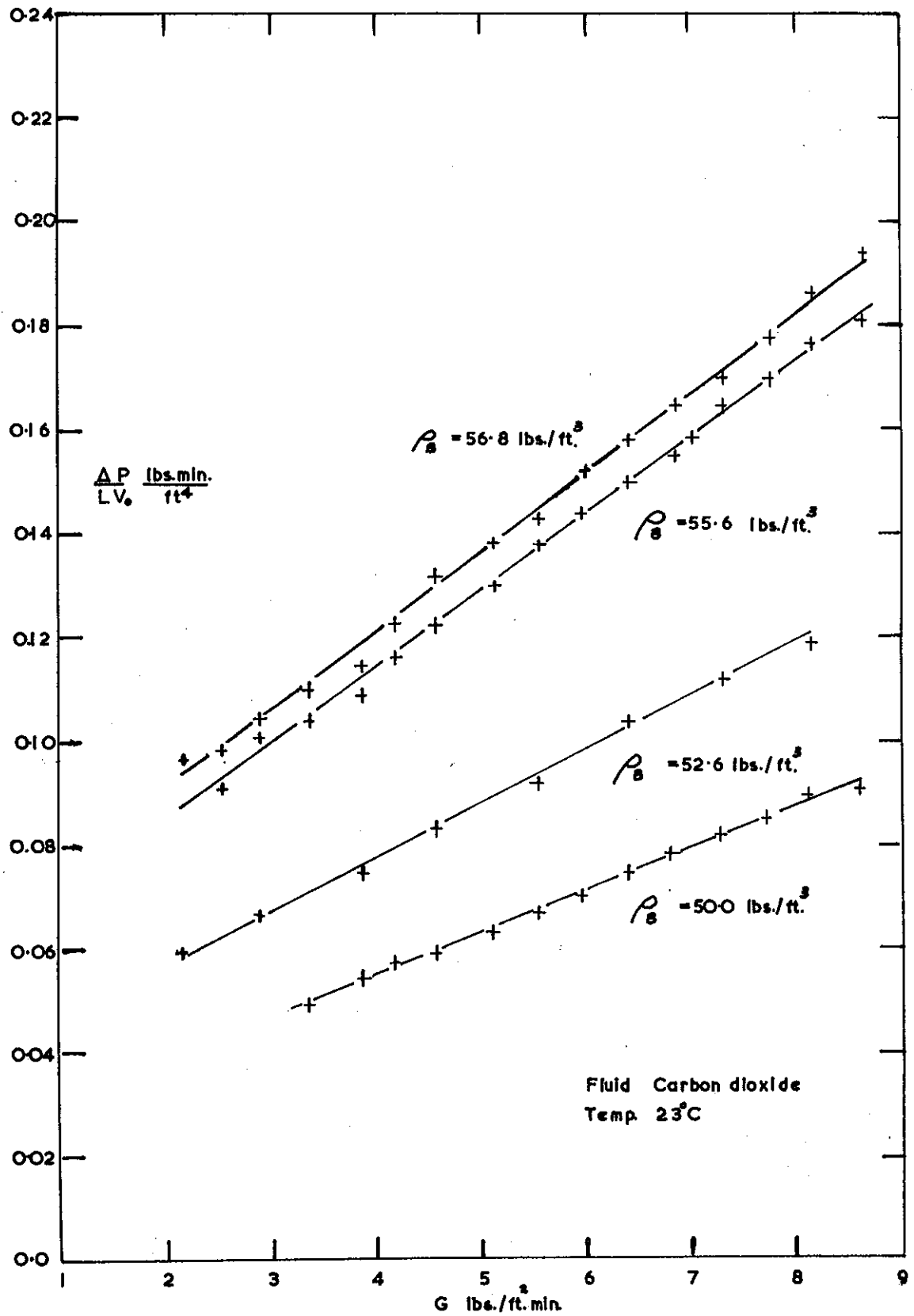


FIG. 13

PLOT  $\frac{\Delta P}{LV_0}$  VERSUS G FOR -5 +6 MESH ALUMINA.

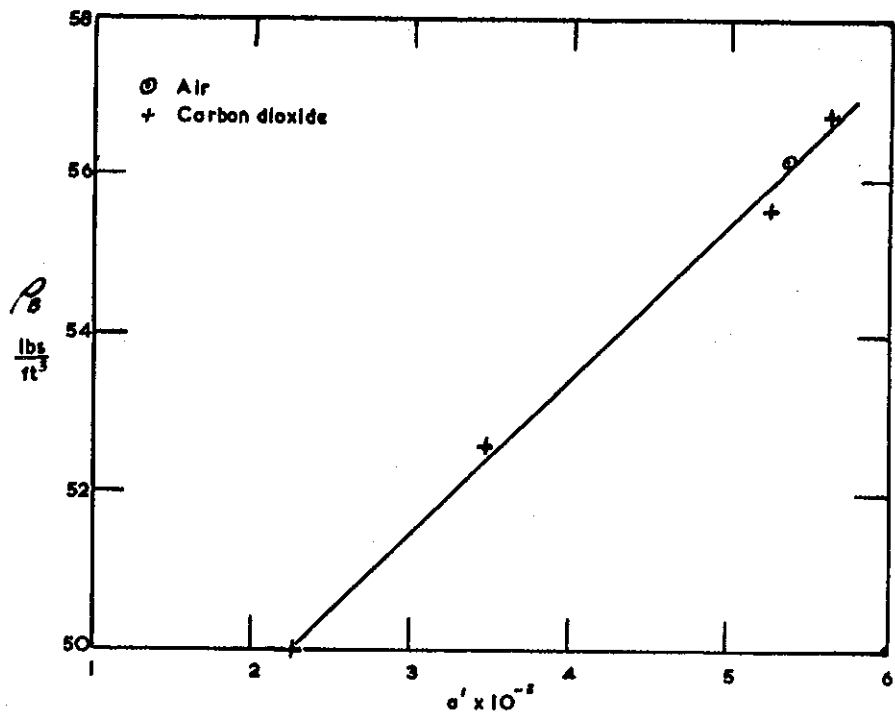


FIG. 14  
 VARIATION of  $a'$  WITH BULK DENSITY for ALUMINA -5+6 MESH

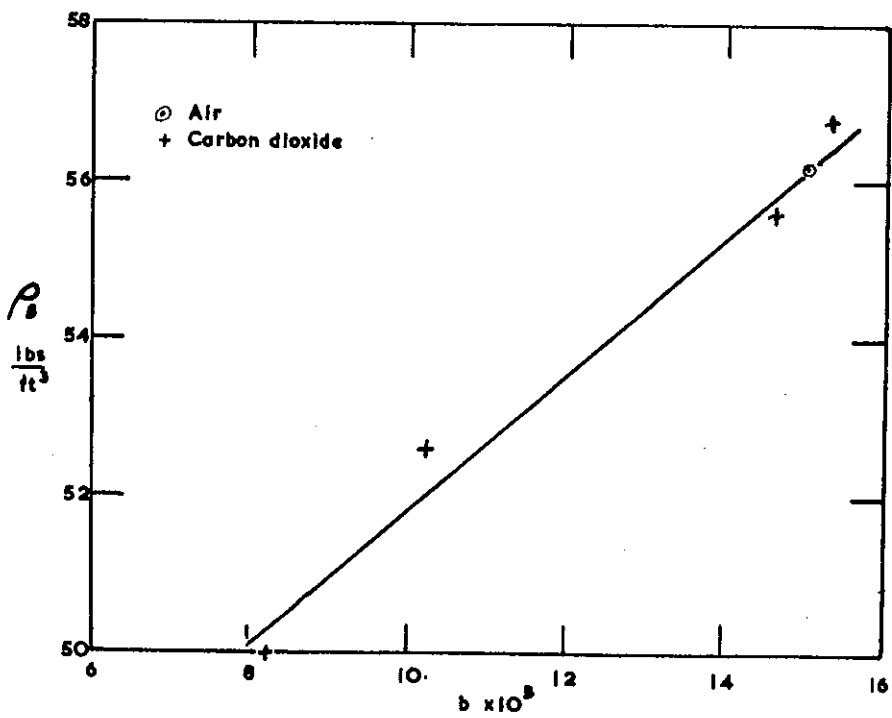


FIG. 15  
 VARIATION of  $b$  WITH BULK DENSITY for ALUMINA -5+6 MESH

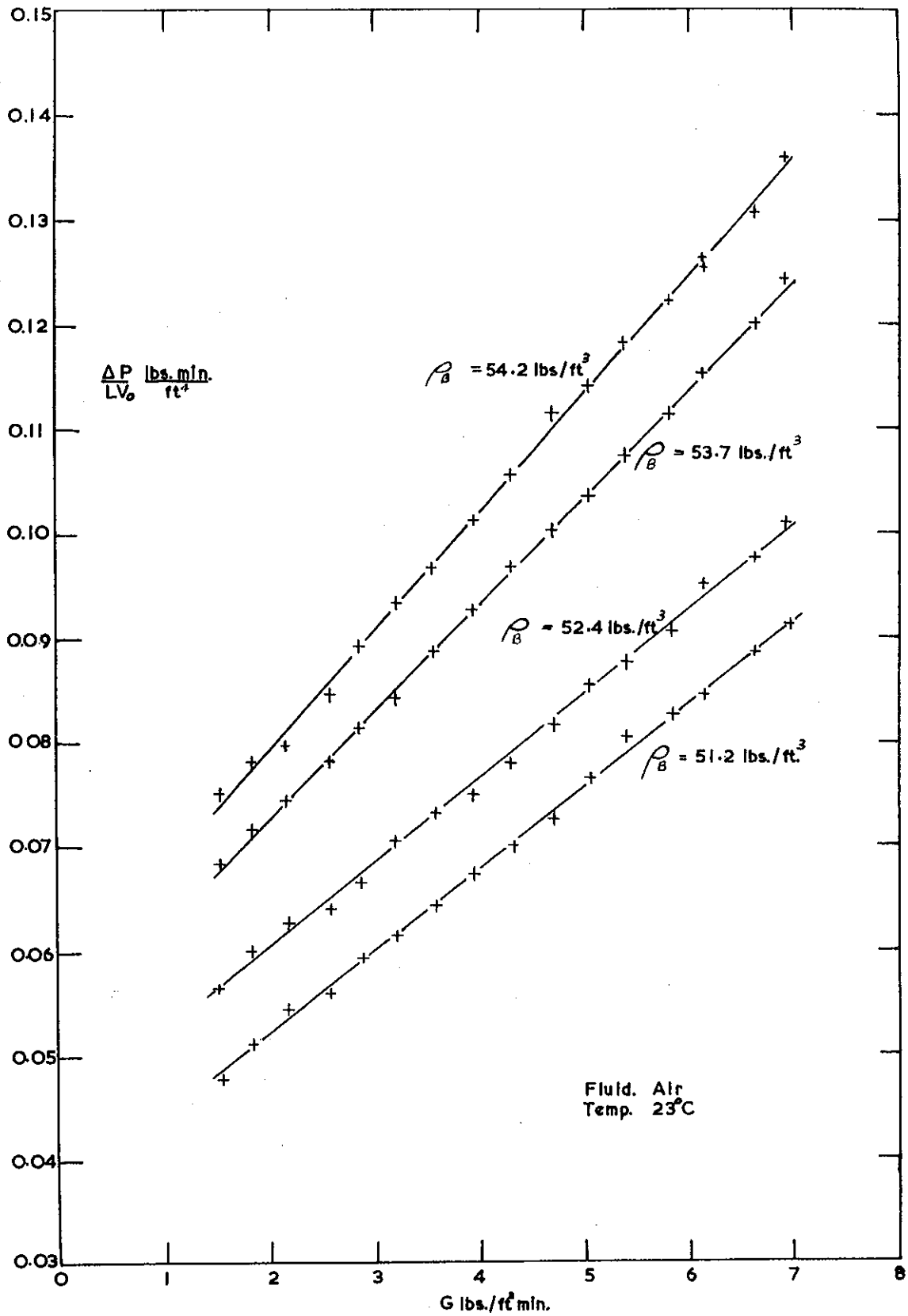


FIG. 16

PLOT  $\frac{\Delta P}{LV_0}$  VERSUS  $G$  FOR  $\frac{3}{16}$  + 5 MESH ALUMINA.

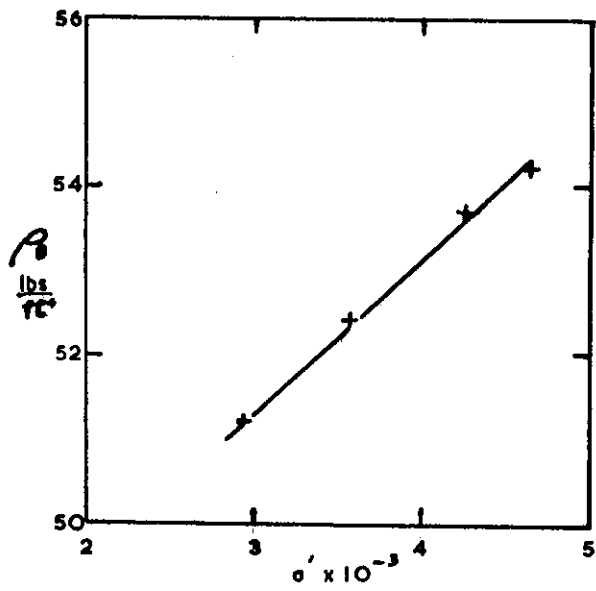


FIG. 17

VARIATION of  $\sigma'$  WITH BULK DENSITY for ALUMINA  $-\frac{3}{16} + 5$  MESH

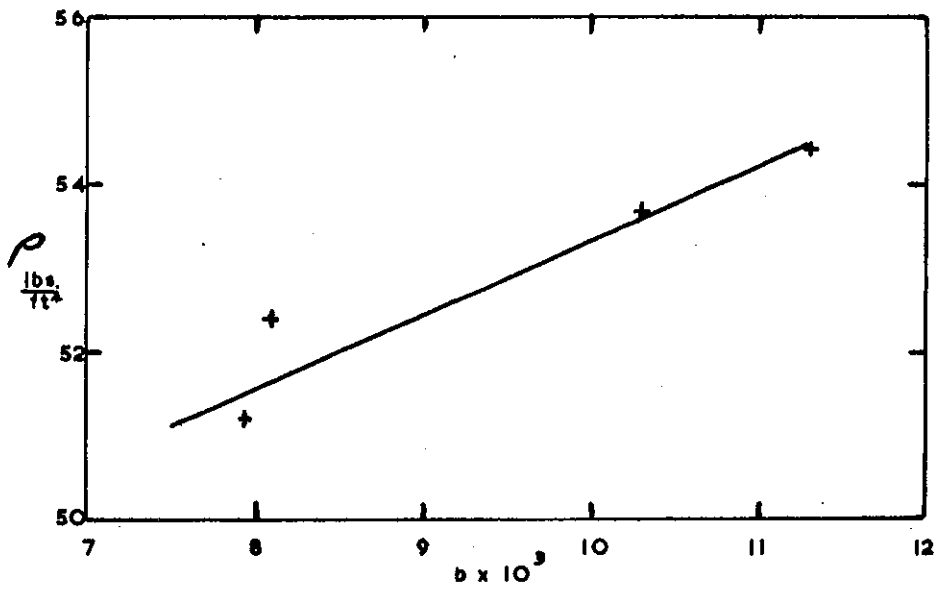


FIG. 18

VARIATION of  $b$  WITH BULK DENSITY for ALUMINA  $-\frac{3}{16} + 5$  MESH.

